Modeling approaches to brushless DC permanent-magnet generator for use in micro-wind turbine applications

Andreea Adriana Laczko (Zaharia), S. Brisset and M.M. Radulescu

***Abstract* -- This paper reports on the modelling of a direct-driven brushless DC permanent-magnet (BLDCPM) generator to be used in micro-wind turbine applications for long-term wind-speed profiles. Three models are investigated and confronted in precision and computation time. For power loss calculation of BLDCPM generator operating under large time-scale wind-speed fluctuations, an original barycenter method is applied.**

***Index Terms* -- brushless DC permanent-magnet generator, direct drive, finite-element field analysis, long-term wind-speed profile, trapezoidal back-EMF, wind energy conversion system.**

I. Introduction

BRUSHLESS DC permanent-magnet (BLDCPM) machines operating in generator mode offer several advantages, such as high efficiency over a wide speed range, low maintenance, greater durability, compactness, and higher power density. Moreover, due to the trapezoidal phase back-EMF of the BLDCPM generator, the rectified DC output voltage has reduced pulsations. Such positive features prompt the BLDCPM generator for use in small-scale wind energy conversion systems (WECSs) [1]-[3].

The direct coupling of the BLDCPM generator to the wind turbine compels it to operate under low-speed and high-torque conditions. The downside of the direct-drive technology is reflected in the cost and weight of the wind generator. The purpose is to search for an optimal design solution of the BLDCPM generator in terms of design specifications, that will give as small power losses as possible over a wind-speed cycle with time-span of one year and consequently maximizing the useful power.

This can be achieved through the bias of an optimization process that tries to find the optimal geometrical and electrical parameters of the generator, for further use in micro-wind turbine applications. As the simulation time is of great importance for the optimization process models with high accuracy can evolve it into a time-consuming process, especially when considering optimization over a wind cycle for the minimization or maximization of different quantities. For this purpose, a compromise must be made between the accuracy of the solution and the computation time.

Andreea Adriana Laczko (Zaharia) is with the Technical University of Cluj-Napoca, Cluj-Napoca, Romania and with the Ecole Centrale de Lille, Villeneuve d'Ascq / Lille, France (e-mail: Andreea.Laczko@mae. utcluj.ro)

S. Brisset is with the Ecole Centrale de Lille, Villeneuve d'Ascq / Lille, France (e-mail: stephane.brisset@ec-lille.fr)

M.M. Radulescu is with the Technical University of Cluj-Napoca, Cluj-Napoca, Romania (e-mail: Mircea.Radulescu@emd.utcluj.ro)

Three techniques are investigated in this paper for the modeling of the BLDCPM generator: analytical, semi-analytical and numerical. The finite element (FE)–based numerical model, which is based on transient magnetic field analysis of the generator by taking into account the rotor motion, the electromagnetic nonlinearities and the hysteresis current control, reveals high accuracy but under penalty of lengthy computation time.

On the other hand, the semi-analytical model, faster in computation time than the FE model is still dependent on a basic sampling time for neatness in the simulation results, neglects the electromagnetic properties of the machine and can only compute global quantities. Lastly, the analytical model is a static one that does not compute waveforms but only peak or mean values. This is the fastest but roughest model.

The aim of this paper is to pave the way for the future design optimization process by determining a reduced-order analytical model of the BLDCPM generator that can be used in its design optimization for operation under very large wind-speed profile. Also, a long-term wind-speed profile partition technique based on barycenter method, allowing fast exploitation of the available data from the wind-speed profile, is proposed and discussed in terms of generator power losses. The design characteristics and electrical parameters of the BLDCPM generator considered in this paper are those fully described in references [4] and [5].

II. Modelling of BLDCPM micro-wind generator

A. Long-term wind-speed profile and turbine model

Typically, a wind-speed profile consists of a large set of data measurements as shown in Fig.1. The data considered for this paper represent the mean value taken over one hour of wind measurements, every hour for one year, resulting in 8759 of measurements that describe the wind behavior.

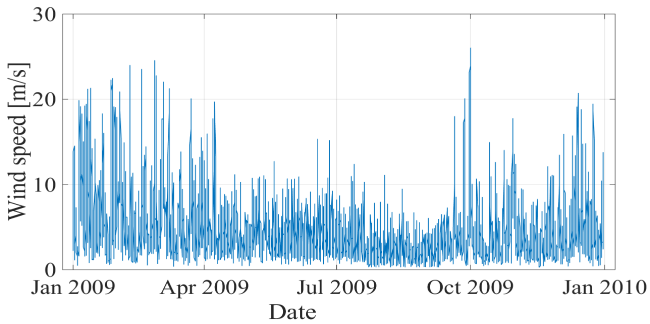

Fig. 1. Long-term wind-speed profile representation

978-1-5090-2537-4/16/$31.00 ©2016 IEEE

The three-blade wind turbine model, delivers power (Fig. 2) expressed as [9]:

$$P_{wt} = \frac{1}{2}\rho_{air}\,\pi R_{wt}^{2}\,C_p(\lambda)\,v_w^{3} \tag{1}$$

where ρ_{air} is the air density (kg/m^3), R_{wt} is the radius of the turbine-rotor blades (m), v_w, the wind speed (m/s), and $C_p(\lambda)$, the power coefficient of the turbine, which corresponds to the turbine studied in [8] and can be found through interpolation as presented in the appendix.

The cut-in speed of the wind represents the start-up of the turbine and the beginning of the wind power extraction until the wind speed reaches its rated value. For wind speeds outrunning this rated value, the turbine is kept to operate at its nominal power by means of different control techniques. When the cut-off wind speed is finally reached, the turbine ceases power generation through its shut-down, for mechanical damage protection.

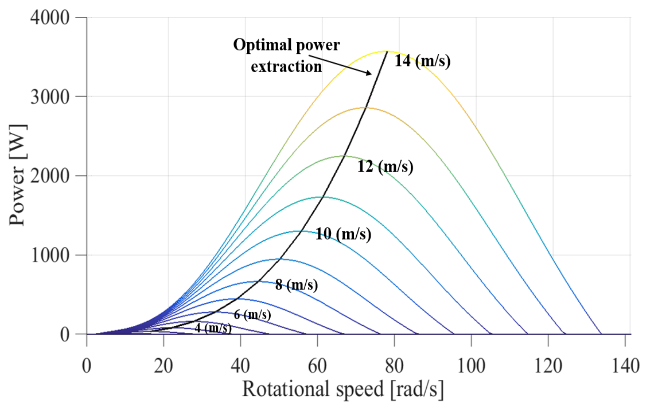

Fig. 2. Power characteristics of the reference micro-wind turbine

B. Semi-analytical model of the BLDCPM generator

The first model to investigate is the time based model. The following phase circuit model for the direct-driven BLDCPM generator having three-phase, star-connected with isolated neutral point stator windings is considered [2], [6]:

$$v - v_n = Ri + (L - M)\frac{di}{dt} + e \tag{2}$$

where R and L are the phase resistance and self-inductance, M is the mutual phase inductance, i and e represent the phase current and back-EMF and v_n is the stator neutral voltage:

$$v_n = \frac{1}{3}\left(\sum v_{abc} - \sum e_{abc}\right) \tag{3}$$

The trapezoidal phase back-EMF waveforms are dependent on the rotational angular speed of the generator, and shifted in all the three stator phases as in Fig. 3.

The electromagnetic torque can be expressed as:

$$T_{em} = \frac{e_a i_a + e_b i_b + e_c i_c}{\Omega} \tag{4}$$

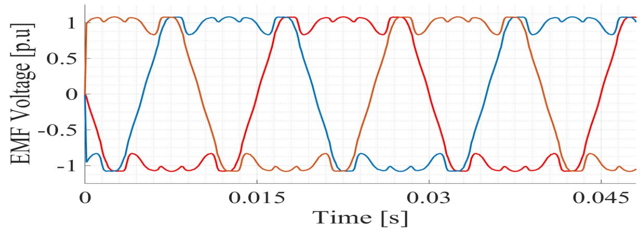

Fig. 3. FE-computed back-EMF waveforms of the considered BLDCPM micro-wind generator

The BLDCPM generator model is implemented in MATLAB/SIMULINK environment for the overall WECS with the schematic representation of Fig.4. The reference power is compared to the power of the system and processed by means of a PI controller. The output of this power-regulation block is used for determining the phase reference currents based on the BLDCPM generator switching pattern dependent on rotor angular position. Hysteresis control of stator phase currents is considered to obtain the driving signals for rectifier power devices and for providing the line-to-neutral stator-phase voltages.

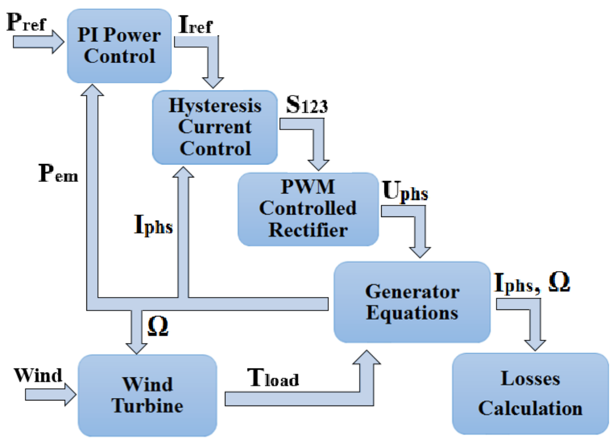

Fig. 4. Simulation model scheme of the direct-driven BLDCPM micro-wind generator under study

Particular quantities, such as the torque ripple and current peak, play a significant part in the design process of the generator. As they are different for each wind speed, in order to see the behavior of the entire system, the wind-speed cycle of 8759 measurements is set as input for the simulation model of the BLDCPM generator and a steady state simulation of one electrical period is carried out for each wind speed in the cycle.

Even before starting the simulation one can presume that it will take a lot of time. That is true, since a fairly large CPU time of 11 hours is needed to perform this type of simulation using MATLAB/SIMULINK software, for basic time-step of 1μs. Hence, considerable time-span is needed in order to use these data together with WECS model in an optimization process that would evaluate them alongside of other design variables for thousands of iterations. Such a strategy is not reasonable, so that the focus should be drifted towards the BLDCPM generator and wind-speed cycle reduced-order models.

C. Long-term wind-speed profile partition by barycenter method

A first attempt in the direction presented above is to maintain the semi-analytical model and find a solution to handle the simulation time over the wind-speed profile. Since through the design optimization of the BLDCPM generator high efficiency is pursued, loss minimization during the wind-speed cycle is required. It should be noted that for this paper, only the copper and the iron losses are taken into discussion.

A first method of determining the power losses of the entire wind cycle is by using each operating point for their calculation. As stated previously, this approach is not adequate due to the large computation time that it requires.

The second method for the losses calculation is based on the barycenter method, which allows to reduce both the simulation time and the wind data that will be considered for the design of the generator. A description of this method was reported in [10], where it was used to reduce the torque and speed driving cycles in the design optimization of an axial-flux traction motor.

This barycenter method is adapted here to the WECS for processing the large amount of wind-speed data. In order to reduce the computation time, the totality of operating points within the wind-speed cycle are replaced with a low number of regions, (Fig.5), whose barycenter are represented by the parameters from (5). These parameters are used for the losses calculation of each region *r*.

$$Bary_r = \begin{cases} \langle v_w \rangle_r, & \text{mean wind speed} \\ \langle v_w^2 \rangle_r, & \text{mean square wind speed} \\ \langle v_w^4 \rangle_r, & \text{mean wind speed of 4th power} \\ N_{pt} & \text{number of points in the region } r \end{cases} \quad (5)$$

The copper loss $P_{j,}$ and iron loss P_{Fe_hys} and P_{Fe_eddy} for each barycenter are calculated as:

$$P_{j,r} = 3 R I_{RMS,r}^2 N_{pt} \frac{\langle v_w^4 \rangle_r}{\langle v_w \rangle_r^4} \quad (6)$$

$$P_{Fe\_hys,r} = k_{hys} \frac{N_p}{2\pi} (B_{th}^{\alpha} + B_{sy}^{\alpha})\, \Omega_r N_{pt} \frac{\langle v_w \rangle_r}{\langle v_w \rangle_r} \quad (7)$$

$$P_{Fe\_eddy,r} = k_{eddy} \frac{N_p^2}{\pi^3} (B_{th}^2 + 2B_{sy}^2)\, \Omega_r^2 N_{pt} \frac{\langle v_w^2 \rangle_r}{\langle v_w \rangle_r^2} \quad (8)$$

A more detailed explanation on the entire process of how these losses equations were determined can be found in the appendix.

To validate the method, at the first step the copper and iron losses of the BLDCPM wind generator were calculated for all points of the wind cycle by using the semi-analytical model and the totality of each loss was obtained through their addition.

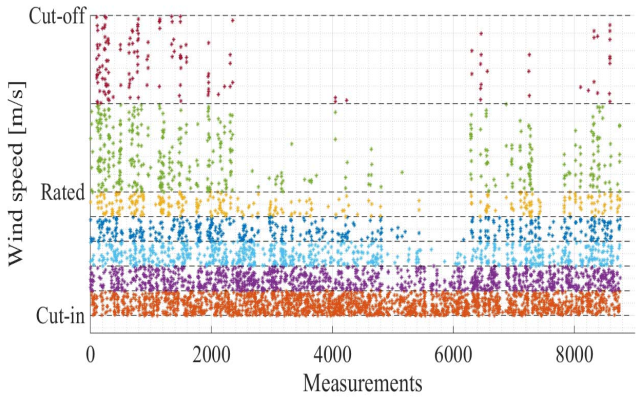

Fig. 5. Division example of a long-term wind-speed profile into a chosen number of regions

The second step was to compute the losses with the help of the same semi-analytical model by applying the barycenter method and the relations (6)-(8), considering a certain number of regions. A relative error was then calculated between the values obtained at the first step and those from the second step and presented in Figs. 6 and 7 with and without taking into account the ratio of the barycenter parameters. The curves in the figures show that the usage of the barycenter ratio allows to achieve a small error faster and with fewer regions.

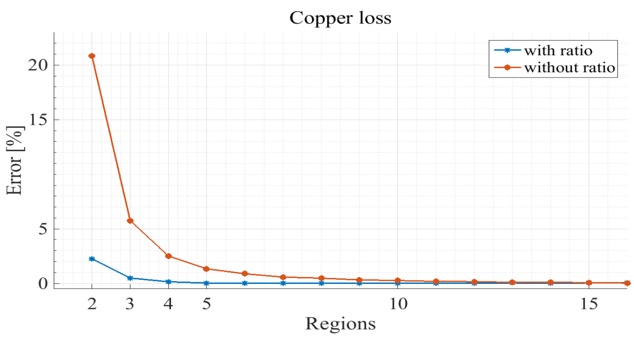

Fig. 6. Percentage errors between calculated copper losses of the considered BLDCPM generator

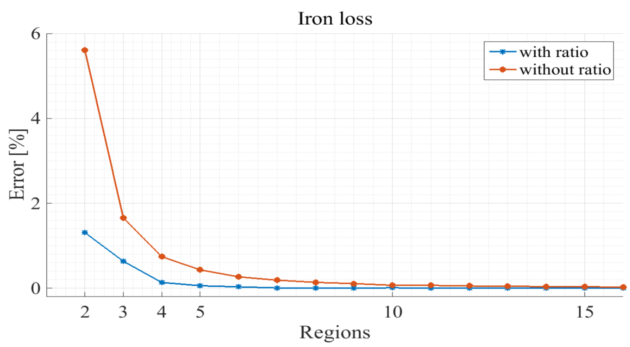

Fig. 7. Percentage errors between calculated iron losses of the considered BLDCPM generator

D. Analytical model of the BLDCPM generator

The second approach is to preserve the wind cycle and instead reduce the semi-analytical model. To develop an analytical model of the BLDCPM wind generator, the time-based characteristics of the above described model have to be discharged and reshaped for faster usage. This new model is based on the circuit equations written by considering only the amplitude of the involved quantities. The rotational speed of the generator, being a linear function of the wind speed, it can easily be computed based on the tip-speed ratio equation:

$$\lambda = \Omega R_{wt} / v_w \tag{9}$$

The electromagnetic power of the generator (P_{em}) is assumed to result as:

$$P_{em} = \begin{cases} 0, & v_w < v_{in},\ v_w \geq v_{max} \\ \dfrac{\pi}{2} \rho_{air} R_{wt}^5 \dfrac{C_{p\,opt}}{\lambda_{opt}^3} \Omega^3 - P_{mech}, & v_{in} \leq v_w \leq v_b \\ P_r - P_{mech}, & v_b < v_w < v_{max} \end{cases} \tag{10}$$

where P_r defines the rated power, v_{in}, v_b, v_{max} represent the cut-in, base and cut-off wind speeds and P_{mech} represents the mechanical loss as [8]:

$$P_{mech} = f_{wt}\, \Omega^2 \tag{11}$$

Due to the fact that the back EMF is proportional to the rotational speed, its amplitude is sufficient to be taken into account for the calculation of the generator phase-stator current peak value:

$$E = k_e \Omega \tag{12}$$

$$I = \frac{P_{em}}{2E} \tag{13}$$

Furthermore, the developed electromagnetic torque can be computed as:

$$T_{em} = 2 k_e I \tag{14}$$

The main advantage of this model resides in the fast evaluation time, which is less than one second for the 8759 wind speed measurements, whereas its drawbacks consist in its inability to predict the current and torque ripples.

E. FE-based numerical model of the BLDCPM generator

As the non-linearity, the geometry and mechanical movement are not considered by neither one of the previous (the semi-analytical and analytical) models and to ensure a certain accuracy of the system a third model is being investigated and that is the FE-based numerical model.

FE-discretized cross-sectional model of the BLDCPM generator (Fig. 8) was created and subjected to numerical field analysis by means of JMAG Designer software [11].

This model was used only for evaluating the simulation performances in precision and computing time of the previous models of the BLDCPM wind generator.

FE simulations were performed for 2-D time-stepping transient field analysis of the BLDCPM wind generator, operating at rated speed of 490 [rpm] (equivalent to 9 [m/s] wind speed) for supplying an isolated rectifier load. The obtained stator-winding phase-current and electromagnetic torque waveforms are presented in Figs. 9 and 10.

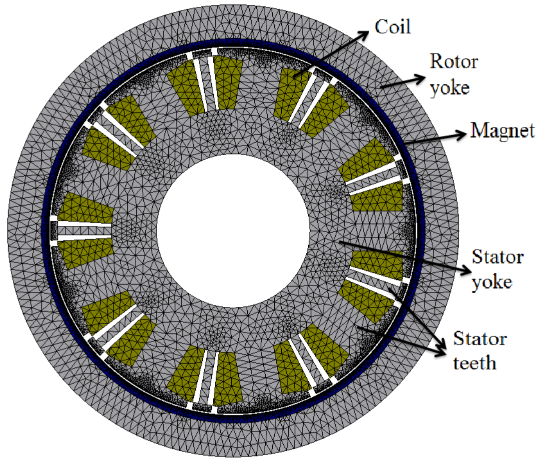

Fig. 8. FE-discretized cross-sectional model of the considered BLDCPM generator

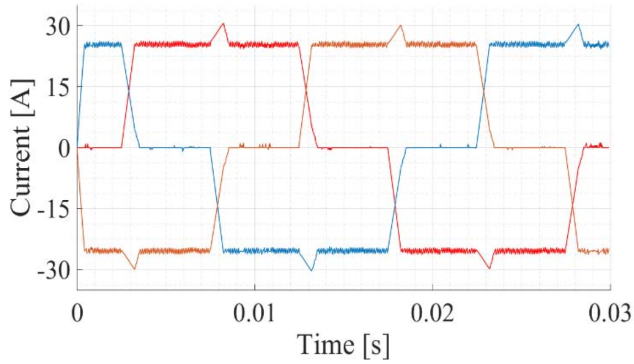

Fig. 9. FE-computed three-phase stator-current waveforms of the considered BLDCPM generator

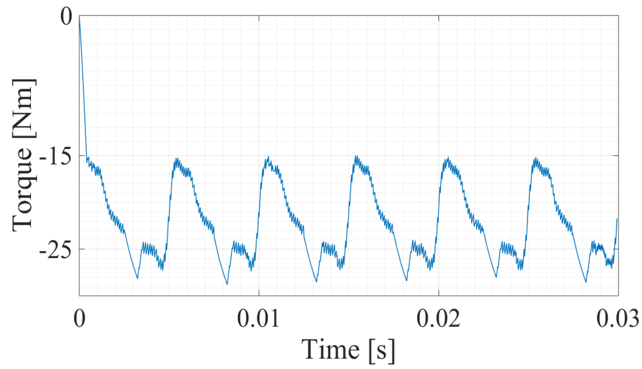

Fig. 10. FE-computed electromagnetic torque waveform of the considered BLDCPM generator

As it can be seen from the above figures a peak in the current waveforms results into an additional ripple in the electromagnetic torque. An average torque error between the (i) numerical and analytical models (orange rhomb) and (ii) numerical and semi-analytical models (red circle), as well as a maximum current error obtained likewise are represented in Fig. 11 alongside the CPU computation time, for the base operating point. Whereas the CPU time necessary for one FE simulation of one operating speed of the wind profile is of 1h and 20 minutes, estimation for the entire long-term wind profile gives one year of simulation time.

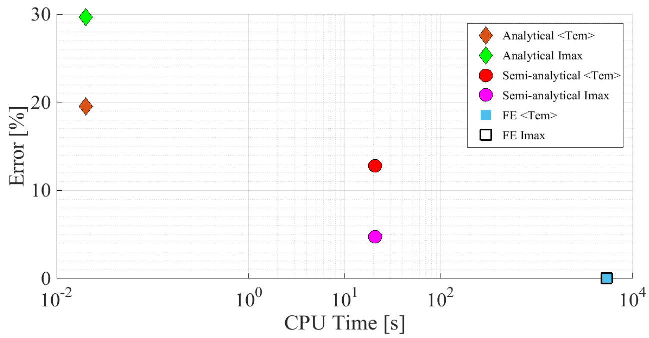

Fig. 11. Errors for average electromagnetic torque and maximum current in FE, semi-analytical, analytical models vs. CPU time in log-scale

A comparative analysis of the FE-computed and analytically-obtained average electromagnetic torque results for different operating points was carried out and reported in Fig.12. The low rotational speed of the turbine at low wind speeds resides in a larger error between the torque quantities of the models. As the wind speed and consequently the rotational speed of the turbine increase the tendency of the error is to decrease and stabilize at a certain value representing the error difference between the analytical and FE models. However, due to the peak in the current waveform, instantly transmitted to the torque curve, the direction of the error changes, as seen in Fig. 12.

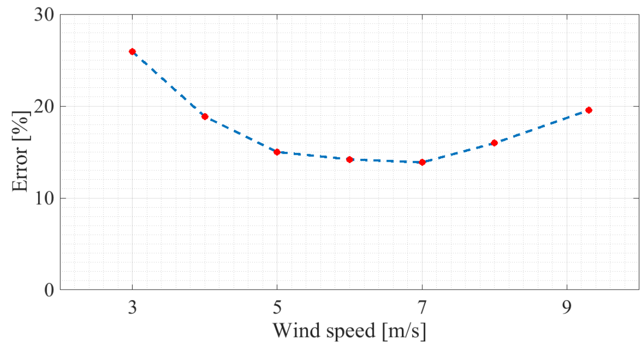

Fig. 12. Error between FE-computed and analytically-obtained electromagnetic torque results vs. wind speed

This rises several constraints to be imposed to the design optimization process in order to achieve the desired performances. Still, regardless of the waveforms of the currents or torque, a significant difference can be observed between the two models, hence, a correction of the analytical model should be effected if considered to be used in design optimization. The same principle is assumed for the semi-analytical model as well.

III. Conclusions

In this paper, a reduced-order analytical model is developed for BLDCPM generator in micro-wind turbine applications under wind-speed cycle constraints. The model can be used in design optimization of the generator operating under very large wind-speed profile. Withal, a wind-speed cycle partition technique based on barycenter method, allowing easy exploitation of large amount of available data from the wind-speed profile, is proposed and discussed in terms of copper and iron losses of the BLDCPM generator. At last, models performances in terms of accuracy and computation time were confronted against finite element-based numerical field model of the considered BLDCPM wind generator.

IV. Appendix

A. *Reference wind turbine parameters*

Radius of the turbine-rotor blades: $R_{wt} = 1.25$ [m]
Friction coefficient: $f_{wt} = 0.02$ [Nm/rad]
Optimal power coefficient: $C_{p\_opt} = 0.441$
Optimal tip speed ratio: $\lambda_{opt} = 6.9$

The Cp (λ) power coefficient of the reference wind turbine is a function of tip speed ratio (λ) and can be found through interpolation:

$C_p(\lambda) = -3.98\cdot10^{-8} \cdot \lambda 7 - 4.21\cdot10^{-6} \cdot \lambda^6 + 2.1\cdot10^{-4} \cdot \lambda^5 - 3.1\cdot10^{-3} \cdot \lambda^4 + 1.64\cdot10^{-2} \cdot \lambda^3 - 0.0176 \cdot \lambda^6 + 0.0174 \cdot \lambda - 1.93\cdot10^{-3}$

where λ depends on the turbine rotational speed, Ω and on the wind speed, v_w as in (9).

B. *Barycenter method*

The copper loss P_j, as a time-varying function, can be expressed for the semi-analytical model as:

$$P_j(t) = R\left[i_a^2(t) + i_b^2(t) + i_c^2(t)\right] \qquad (15)$$

From (15) the average copper loss can be found by determining the RMS value of one period ($0 \le t \le T$) of the function through relations (16)-(19):

$$P_j = \langle P_j(t)\rangle_T = \frac{1}{T}\int_0^T P_j(t)dt \qquad (16)$$

$$P_j = \frac{R}{T}\int_0^T \left[i_a^2(t) + i_b^2(t) + i_c^2(t)\right]dt \qquad (17)$$

$$P_j = R\left[\frac{1}{T}\int_0^T i_a^2(t)dt + \frac{1}{T}\int_0^T i_b^2(t)dt + \frac{1}{T}\int_0^T i_c^2(t)dt\right] \qquad (18)$$

$$P_j = R\left[I_{RMS\_a}^2 + I_{RMS\_b}^2 + I_{RMS\_b}^2\right] \qquad (19)$$

where $I_{RMS\_ph} = \sqrt{\frac{1}{T}\int_0^T i_{ph}^2(t)dt}$ represents the equation which determines the quadratic mean for each phase current. Assuming that the phase currents have the same RMS value the losses in the stator windings become:

$$P_j = 3R\, I_{RMS}^2 \qquad (20)$$

From the turbine power equation it is assumed that the electromagnetic power of the BLDCPM generator is proportional to the cube of the wind speed, whereas its rotational angular speed, Ω, is linked to the wind speed by relation (21). Therefore, the torque can be also considered proportional to the square wind speed as in (22) and linked to the RMS current by (23):

$$\Omega = k_s v_w \tag{21}$$

$$T_{em} = k_w v_w^2 \tag{22}$$

$$T_{em} = k_t I_{RMS} \tag{23}$$

where k_s, k_t, k_w are speed and torque coefficients.

In this context, (20) becomes:

$$P_j = k_j v_w^4 \tag{24}$$

where $k_j = 3R\left(k_w / k_t\right)^2$. Assuming k_j is constant within one region, then the sum of copper loss for all the points (p) in the considered region (r) can be written as:

$$\sum_{p=1}^{Npt} P_{j,p} = k_{j,r} \sum_{p=1}^{Npt} v_{w,p}^4 = k_{j,r}\, N_{pt} \left\langle v_w^4 \right\rangle_r \tag{25}$$

As $k_{j,r}$ is constant, it can be computed for any point of the region, but the barycenter of the considered area is preferred:

$$k_{j,r} = \frac{P_{j,b}}{v_{w,b}^4} = \frac{3RI_{RMS,b}^2}{v_{w,b}^4} = \frac{3RI_{RMS,r}^2}{v_{w,r}^4} \tag{26}$$

with $v_{w,b} = \left\langle v_w \right\rangle_r$ and $I_{RMS,b} = I_{RMS,r}$ its corresponding current, computed for the wind speed $v_{w,b}$.

Finally,

$$P_{j,r} = \sum_{p=1}^{Npt} P_{j,p} = \frac{3RI_{RMS,r}^2}{v_{w,r}^4} N_{pt} \left\langle v_w^4 \right\rangle_r \tag{27}$$

$$P_{j,r} = 3RI_{RMS,r}^2 N_{pt} \frac{\left\langle v_w^4 \right\rangle_r}{\left\langle v_w \right\rangle_r^4} \tag{28}$$

and it is based on $I_{RMS,r}$, $<v_w>_r$, $<v^4_w>_r$ to be computed.

The iron losses in the stator core of the BLDCPM wind generator can be computed in terms of hysteresis and eddy current losses [7] as:

$$\begin{aligned} P_{Fe\_hys} &= k_{hys}\ f\ (B_{th}^{\alpha} + B_{sy}^{\alpha}) \\ P_{Fe\_eddy} &= \frac{4}{\pi} k_{eddy}\ f^2\ (B_{th}^2 + 2B_{sy}^2) \end{aligned} \tag{29}$$

where B_{th}, B_{sy} are the stator tooth and yoke flux densities, and k_{hys} and k_{eddy} represent the hysteresis and eddy current loss coefficients, which can be calculated from manufacturer data, and f is the electrical frequency, which is given by the pole-pairs number and by the rotor angular speed of the machine:

$$\omega_e = N_p\, \Omega, \qquad \omega_e = 2\pi f \tag{30}$$

In this context, (29) becomes:

$$\begin{aligned} P_{Fe\_hys} &= k_{hys}\ \frac{N_p}{2\pi}\ (B_{th}^{\alpha} + B_{sy}^{\alpha})\ \Omega \\ P_{Fe\_eddy} &= k_{eddy}\ \frac{N_p^2}{\pi^3}\ (B_{th}^2 + 2B_{sy}^2)\ \Omega^2 \end{aligned} \tag{31}$$

Given also the proportionality of the rotor angular speed of the machine to the wind speed:

$$\begin{aligned} P_{Fe\_hys} &= C_{hys}\ v_w \\ P_{Fe\_eddy} &= C_{eddy}\ v_w^2 \end{aligned} \tag{32}$$

where $C_{hys} = k_s k_{hys} \frac{Np}{2\pi}(B_{th}^{\alpha} + B_{sy}^{\alpha})$ and $C_{eddy} = k_s^2 k_{eddy} \frac{Np^2}{\pi^3}(B_{th}^2 + 2B_{sy}^2)$.

Assuming C_{hys} *and* C_{eddy} are constant within one region then the sum of iron loss for all the points (p) in the considered region (r) can be written as:

$$\begin{aligned} \sum_{p=1}^{Npt} P_{Fe\_hys,p} &= C_{hys,r} \sum_{p=1}^{Npt} v_{w,p} = C_{hys,r}\ N_{pt} \left\langle v_w \right\rangle_r \\ \sum_{p=1}^{Npt} P_{Fe\_eddy,p} &= C_{eddy,r} \sum_{p=1}^{Npt} v_{w,p}^2 = C_{hys,r}\ N_{pt} \left\langle v_w^2 \right\rangle_r \end{aligned} \tag{33}$$

As C_{hys} and C_{eddy} are constant, they can be computed for any point of the region, but the barycenter of the considered area is preferred:

$$\begin{aligned} C_{hys,r} &= \frac{P_{Fe\_hys,b}}{v_{w,b}} = \frac{k_{hys}\ \frac{N_p}{2\pi}\ (B_{th}^{\alpha} + B_{sy}^{\alpha})\ \Omega_b}{v_{w,b}} \\ &= \frac{k_{hys}\ \frac{N_p}{2\pi}\ (B_{th}^{\alpha} + B_{sy}^{\alpha})\ \Omega_r}{v_{w,r}} \\ C_{eddy,r} &= \frac{P_{Fe\_eddy,b}}{v_{w,b}^2} = \frac{k_{eddy}\ \frac{N_p^2}{\pi^3}\ (B_{th}^2 + 2B_{sy}^2)\ \Omega_b^2}{v_{w,b}^2} \\ &= \frac{k_{eddy}\ \frac{N_p^2}{\pi^3}\ (B_{th}^2 + 2B_{sy}^2)\ \Omega_r^2}{v_{w,r}^2} \end{aligned} \tag{34}$$

with $v_{w,b} = \left\langle v_w \right\rangle_r$ and $\Omega_b = \Omega_r$ its corresponding rotational speed, computed for the wind speed $v_{w,b}$.

Finally,

$$P_{Fe\_hys,r} = \sum_{p=1}^{Npt} P_{Fe\_hys,p} = \frac{k_{hys}\ \frac{N_p}{2\pi}\ (B_{th}^{\alpha} + B_{sy}^{\alpha})\ \Omega_r}{v_{w,r}} N_{pt} \langle v_w \rangle_r \tag{35}$$

$$P_{Fe\_hys,r} = k_{hys}\ \frac{N_p}{2\pi}\ (B_{th}^{\alpha} + B_{sy}^{\alpha})\ \Omega_r\ N_{pt} \frac{\left\langle v_w \right\rangle_r}{\left\langle v_w \right\rangle_r} \tag{36}$$

$$P_{Fe\_eddy,r} = \sum_{p=1}^{Npt} P_{Fe\_eddy,p} = \frac{k_{eddy}\ \frac{N_p^2}{\pi^3}\ (B_{th}^2 + 2B_{sy}^2)\ \Omega_r^2}{v_{w,r}^2} N_{pt} \langle v_w^2 \rangle_r \tag{37}$$

$$P_{Fe\_eddy,r} = k_{eddy}\ \frac{N_p^2}{\pi^3}\ (B_{th}^2 + 2B_{sy}^2)\ \Omega_r^2\ N_{pt} \frac{\left\langle v_w^2 \right\rangle_r}{\left\langle v_w \right\rangle_r^2} \tag{38}$$

and it is based on Ω_r, $<v_w>_r$, $<v_w^2>_r$ to be computed.

V. REFERENCES

[1] R. Krishnan, G.-H. Rim, “Modeling, simulation, and analysis of variable-speed constant frequency power conversion scheme with a permanent magnet brushless DC generator”, *IEEE Trans. Ind. Electron.*, Vol. 37, No. 4, 1990, pp. 291 – 296.

[2] H.-W. Lee, T.-H. Kim, M. Ehsani, “Practical control for improving power density and efficiency of the BLDC generator”, *IEEE Trans. Power Electron.*, Vol. 20, No. 1, 2005, pp. 192-199.

[3] B. Singh, S. Sharma, ”PMBLDCG based stand-alone wind energy conversion system for small scale applications*”, International Journal of Engineering, Science and Technology*, Vol. 4, No. 1, 2012, pp. 65-73A.

[4] T.J.E. Miller, J.R. Hendershot Jr., “Design of Brushless Permanent-Magnet Motors”, *Magna Physics Publishing and Clarendon Press*, Oxford, UK, 1994.

[5] S. Brisset, P. Brochet, “Analytical model for the optimal design of a brushless DC wheel motor”, *COMPEL*, Vol. 24, No. 3, 2005, pp. 829-848.

[6] Andreea Laczko, M.V. Zaharia, M.M. Radulescu, S. Brisset, “Modeling and simulation of a brushless DC permanent-magnet generator-based wind energy conversion system”, *Proc. Int. Conf. Ecol. Veh. Renew. Energ. – EVER 2015*, 7pp.

[7] P. Andrada, M. Torrent, J.L. Perat, B. Blanque, B., “Power Losses in Outside-Spin Brushless D.C. Motors”, *Rep. Universitat Politecnica de Catalunya,* Barcelona, Spain, 2004.

[8] M. Belouda, A. Jaafar, B. Sareni, X. Roboam, J. Belhadj, “Design methodologies for sizing a battery bank devoted to a stand-alone and electronically passive wind turbine system”, *Renewable and Sustainable Energy Reviews, Elsevier*, 2016, vol. 60, pp. 144-154.

[9] J.F. Manwell, J.G. McGowan, A.L. Rogers,”Wind Energy Explained: Theory, Design and Application”, *John Wiley & Sons Publication*, New York, USA, 2009.

[10] G. Krebs, E. de Cecco, C. Marchand, “Design approach of an axial motor for electrical powertrain vehicle”, *Proc. Int. Conf. Electr. Mach. – ICEM 2012*, 6 pp.

[11] www.jmag-international.com.

VI. BIOGRAPHIES

Andreea Adriana Laczko (Zaharia) was born in Romania in 1987. She received the M.Sc. degree from Faculty of Electrical Engineering, Technical University of Cluj-Napoca, Cluj-Napoca, Romania, in 2012. Since October 2012, she pursues a full-time Ph.D. study program in Electrical Engineering at the Technical University of Cluj-Napoca under international co-supervision of Ecole Centrale de Lille, France. Her research interests are in special electric machines for renewable energy applications.

Stephane Brisset is a graduate of Engineer School in 1992 at Ecole Centrale de Lille, France, PhD in Electrical Engineering in 1995 at Université des Sciences et Technologies de Lille. He joined Ecole des Hautes Etudes Industrielles in 1996 and Ecole Centrale de Lille in 2001 where he is now Associate Professor at Laboratoire d’Electrotechnique et d’Electronique de Puissance (L2EP). His main interests are the simulation, design and optimization of electric machines. He is author or co -author of many published scientific papers in refereed technical journals and international conference.

Mircea M. Radulescu received the Dipl.-Ing. degree with honors from the Technical University of Cluj-Napoca, Cluj-Napoca, Romania, in 1978 and the Ph.D. degree from the Polytechnic University of Timisoara, Timisoara, Romania, in 1993, both in electrical engineering. Since 1983, he has been with the Faculty of Electrical Engineering, Technical University of Cluj-Napoca, Romania, where he is currently Full Professor in the Department of Electric Machines and Drives, as well as Head of the Special Electric Machines and Light Electric Traction (SEMLET) Research Laboratory. He is author or co-author of more than 150 published scientific papers in refereed technical journals and international conference and symposium proceedings. His teaching and research activities include classical and special electric machines, computer-aided design of electromechanical devices, design and control of small electronically-commutated motors, actuators and mechatronic drives, light electric traction systems.